BRAIN. Broad Research in Artificial Intelligence and Neuroscience
e-ISSN: 2067-3957 | p-ISSN: 2068-0473
Covered in: Web of Science (ESCI); EBSCO; JERIH PLUS (hkdir.no); IndexCopernicus; Google Scholar; SHERPA/RoMEO; ArticleReach Direct; WorldCat; CrossRef; Peeref; Bridge of Knowledge (mostwiedzy.pl); abcdindex.com; Editage; Ingenta Connect Publication; OALib; scite.ai; Scholar9; Scientific and Technical Information Portal; FID Move; ADVANCED SCIENCES INDEX (European Science Evaluation Centre, neredataltics.org); ivySCI; exaly.com; Journal Selector Tool (letpub.com); Citefactor.org; fatcat!; ZDB catalogue; Catalogue SUDOC (abes.fr); OpenAlex; Wikidata; The ISSN Portal; Socolar; KVK-Volltitel (kit.edu)
2026, Volume 17, Issue 1, pages: 358-376
Submitted: October 24th, 2025 | *Accepted for publication:* January 23rd, 2026

The Relationship Between Cardiac Adipose Tissue and Anxiety in Bariatric Patients: Deep Learning Applications in Epicardial Adipose Tissue Analysis

Mihaela Toader
Doctoral School, Grigore T Popa University of Medicine and Pharmacy, Iasi, Romania.
mihaela.toaderr@gmail.com

Ana-Maria Buburuz
1th Medical Department, Grigore T Popa University of Medicine and Pharmacy, Iasi, Romania
Cardiology Clinic, St Spiridon County Clinical Emergency Hospital, Iasi, Romania.

Madalina Maxim
Doctoral School, Grigore T Popa University of Medicine and Pharmacy, Iasi, Romania
Department of Surgery, St Spiridon County Clinical Emergency Hospital, Iasi, Romania.

Daniela-Ivona Tomita*
Clinical Department, Apollonia University, Păcurari Street 11, 700511 Iasi, Romania.
daniela.tomita@yahoo.com

Bogdan Novac
Faculty of Medicine, University of Medicine and Pharmacy "Grigore T. Popa", 700115 Iasi, Romania.

Otilia Novac
Faculty of Medicine, University of Medicine and Pharmacy "Grigore T. Popa", 700115 Iasi, Romania.

Daniel Vasile Timofte
Department of Surgery, Grigore T Popa University of Medicine and Pharmacy Iasi, Romania.

Corresponding author: Daniela-Ivona Tomita
Clinical Department, Apollonia University, Păcurari Street 11, 700511 Iasi, Romania
daniela.tomita@yahoo.com

Abstract:
Background: *Obesity affects both physical and mental health, and bariatric patients often show high levels of psychological distress. Cardiac adipose tissue, which includes epicardial and pericardial fat, is an active fat depot linked to inflammation and cardiovascular risk. Its relationship with anxiety has not been well studied, especially in bariatric candidates.*
Methods: *This cross-sectional study included 29 adults undergoing preoperative evaluation for bariatric surgery. All participants completed the Hamilton Anxiety Rating Scale and underwent CT imaging to measure epicardial and pericardial adipose tissue thickness. Additional adiposity measures included BMI, waist circumference, abdominal wall thickness, and adipose tissue density. Correlations and simple linear regressions were used to examine associations between anxiety severity and adiposity markers. Group differences across obesity grades were assessed with one-way ANOVA.*
Results: *Higher anxiety scores were strongly associated with greater pericardial fat thickness ($r = 0.621$, $p < 0.001$), epicardial fat thickness ($r = 0.667$, $p < 0.001$), BMI ($r = 0.840$, $p < 0.001$), waist circumference ($r = 0.748$, $p < 0.001$), and abdominal wall thickness ($r = 0.494$, $p = 0.007$). Both pericardial and epicardial fat thickness significantly predicted Hamilton total score in regression models.*
Conclusion: *Anxiety severity in bariatric patients is closely related to several markers of adiposity, especially cardiac adipose tissue thickness. These findings suggest that cardiac adipose tissue may play a meaningful role in the psychological profile of individuals with severe obesity. Integrating both biological and psychological factors may improve the assessment and care of bariatric candidates.Artificial intelligence, especially deep learning techniques, is starting to play an increasingly important role in the assessment of epicardial and pericardial adipose tissue. It allows for automated segmentation and quantification based on CT images, providing high accuracy and reducing the time required for data processing. Recent artificial intelligence models, such as convolutional neural networks and U-Net architectures, have demonstrated significant agreement with manual measurements performed by specialists, which supports the possibility of their integration into routine clinical assessment. In the case of bariatric patients, these technologies can increase the accuracy of cardiac adipose tissue assessment and facilitate a broader understanding of the relationship between obesity, cardiovascular risk and the associated psychological impact.*

Keywords: bariatric; obesity; anxiety; epicardial adipose tissue; pericardial adipose tissue, artificial intelligence, deep learning, convolutional neural networks

How to cite: Toader, M., Buburuz, A.-M., Maxim, M., Tomita, D.I., Novac, B., Novac, O., & Timofte D.V. (2026). The relationship between cardiac adipose tissue and anxiety in bariatric patients: Deep learning applications in epicardial adipose tissue analysis. *BRAIN. Broad Research in Artificial Intelligence and Neuroscience, 17*(1), 358-376. https://doi.org/10.70594/brain/17.1/25

1. Introduction

Literature defines obesity as a chronic, progressive disease that develops over time. It is characterized by an excessive accumulation of adipose tissue that disrupts the body's normal physiology and increases the risk of various health problems. Obesity remains difficult to manage in the long term, because even when treated, many individuals regain weight over time despite psychological, medical or surgical interventions. Therefore, obesity requires continuous treatment rather than a one-time intervention given its complex emotional, physical and behavioral components. Approximately 890 million adults were living with obesity in 2022, according to the World Health Organization. This means that one in eight people is affected by obesity, and reports demonstrate that the numbers continue to rise each year (World Health Organization, 2021). The observed global rise in obesity prevalence could be explained by sedentarism, reduced physical activity at work and at home, and the widespread availability of inexpensive, highly processed foods that are high in calories and low in important nutrients (Ng et al., 2014). In addition, obesity is associated with a wide range of serious medical conditions, including type 2 diabetes, hypertension, obstructive sleep apnea, non-alcoholic fatty liver disease, and various forms of cancer. Therefore, obesity is now recognized as one of the most critical public health problems worldwide because of its extensive health impact and rapidly increasing prevalence (Guh et al., 2009; Hruby & Hu, 2015).

In addition, the excess adipose tissue is known to promote chronic inflammation, to alter the structure of blood vessels, and to impair the autonomic control of the cardiovascular system. Through these molecular mechanisms, obesity increases the risk of coronary diseases, heart failure, arrhythmia, and other major cardiovascular conditions (Lavie, Milani, & Ventura, 2009; Powell-Wiley et al., 2021). In recent years, the focus of research has shifted to the adipose tissue surrounding the heart. This cardiac fat tissue includes the epicardial adipose tissue and the pericardial adipose tissue. The epicardial adipose tissue is located between the myocardium and the visceral pericardium. On the other hand, the pericardial adipose tissue lies outside the heart, within the pericardial sac. These two adipose tissues are particularly important because they are biologically active and release inflammatory signals that can affect cardiac function and the coronary arteries (Iacobellis, 2015; Mahabadi et al., 2009).

The most reliable method for measuring these types of cardiac adipose tissues is computed tomography. This method provides a clear visualization of the heart and surrounding structures and identifies adipose tissue based on its characteristic density (Rosito et al., 2008). Axial CT images are now used to measure the epicardial and pericardial adipose tissue thickness. These measurements are used as indicators of visceral adiposity and cardiovascular risk. Our research group has previously described and validated the CT methodology used to evaluate these cardiac adipose tissues in clinical practice (Toader et al., 2025).

Obesity is also linked to a range of mental health disorders. Individuals with severe obesity frequently report higher levels of anxiety, a pattern associated with biological factors such as inflammation and hormonal dysregulation, as well as social factors, including stigma and reduced quality of life (Luppino et al., 2010; Gariepy, Nitka, & Schmitz, 2010). Anxiety can be assessed with the Hamilton Anxiety Rating Scale, a clinician-rated instrument that evaluates both psychological and physical symptoms (Hamilton, 1959).

Although many studies have examined the physical and psychological consequences of obesity, the correlation between cardiac adipose tissue and anxiety remains insufficiently explored. Patients who seek bariatric surgery commonly present with severe obesity, increased cardiovascular risk, and elevated levels of various psychological symptoms. Therefore, it is important to understand how cardiac adipose tissue relates to anxiety in these patients. The findings of this study may lead to a better understanding of the biological and emotional factors that influence their overall health.

The aim of this study was to examine the relationship between epicardial and pericardial adipose tissue thickness and anxiety severity in bariatric patients. Our experimental design used CT

measurements combined with a standardized anxiety assessment to provide a clearer picture of the physical and psychological profile of bariatric candidates.

2. Methods

2.1. Study Design and Participants

Our study was cross-sectional and observational. The sample included 29 adult patients undergoing preoperative evaluation for bariatric surgery at a specialized clinical center. All participants completed a standardized psychological assessment and a computed tomography (CT) scan. Eligibility criteria included age of at least 18 years, a completed CT scan, and having undergone the anxiety assessment. All participants with missing imaging or psychometric data were excluded.

2.2. Anxiety Assessment

Anxiety levels were measured using the Hamilton Anxiety Rating Scale. The scale evaluates psychological, somatic, and autonomic symptoms, generating a total anxiety severity score (Hamilton, 1959). Anxiety assessments were performed by trained clinicians during the preoperative visit.

2.3. Evaluation of Cardiac Adipose Tissue using CT

All participants underwent non-contrast CT imaging using a standardized protocol. Cardiac adipose tissue was quantified through two primary measures. Firstly, the epicardial adipose tissue thickness was measured on the right ventricular free wall at the mid-ventricular level. Secondly, the pericardial adipose tissue thickness was assessed anterior to the right ventricle, between the parietal pericardium and the sternum. The measurement protocol followed the technique previously described by our scientific group in an earlier article (Toader et al., 2025). Furthermore, additional adiposity-related variables were also measured for secondary analyses. These measures included abdominal wall thickness and adipose tissue density (Hounsfield units).

2.4. Body composition measures

Standard body composition data was also collected during the preoperative evaluation. The data included body mass index (BMI), waist circumference, height, and weight.

2.5. Statistical Analysis

All statistical analyses were performed using IBM SPSS Statistics, version 26. Descriptive statistics (means, standard deviations, ranges) were calculated for all variables. Normality was assessed using Shapiro-Wilk and visual inspection. Associations between anxiety levels and cardiac adipose tissue were examined using Pearson or Spearman correlation coefficients.

Separate simple linear models of regression were used to analyze whether epicardial adipose tissue thickness, pericardial adipose tissue thickness, BMI and waist circumference can explain the anxiety levels of the participants. All statistical tests were two-tailed, and a p-value < 0.05 was considered statistically significant. Confidence intervals were calculated at 95%. For the regression models, effect sizes were used to report the magnitude of the associations.

3. Results

3.1. Descriptive statistics

The descriptive analysis showed that 89.7 percent of our participants were women and 10.3 percent were men. Mean height was 165.62 cm (SD = 7.18) and mean weight was 105.50 kg (SD = 14.52). BMI averaged 38.43 kg/m² (SD = 4.71), and waist circumference averaged 113.52 cm (SD = 10.61). Adipose tissue density had a mean of −114.62 HU (SD = 6.09). Abdominal wall thickness averaged 52.24 mm (SD = 13.35). Pericardial fat thickness averaged 53.28 mm (SD = 10.05), and epicardial fat thickness averaged 31.76 mm (SD = 3.88).

Hamilton Anxiety Rating Scale scores showed the following means: anxious mood 3.07, tension 2.93, fears 3.62, insomnia 3.00, cognitive symptoms 2.21, depressed mood 3.38, somatic muscular 2.90, somatic sensory 1.93, cardiovascular 3.21, respiratory 2.83, gastrointestinal 2.97, genitourinary 1.66, autonomic 1.55, and behavior at interview 2.97. The total HAM-A score ranged from 28 to 43, with a mean of 38.38 (SD = 3.14).

3.2. Correlation analysis

We used Pearson correlations to measure the linear associations between the Hamilton total score and the adiposity-related variables. The results showed that Hamilton total score was positively associated with pericardial fat thickness ($r = 0.621$, $p < 0.001$) (Figure 1), epicardial fat thickness ($r = 0.667$, $p < 0.001$) (Figure 2), BMI ($r = 0.840$, $p < 0.001$), waist circumference ($r = 0.748$, $p < 0.001$), and abdominal wall thickness ($r = 0.494$, $p = 0.007$). Adipose tissue density was not significantly correlated with the Hamilton total score ($r = –0.250$, $p = 0.191$).

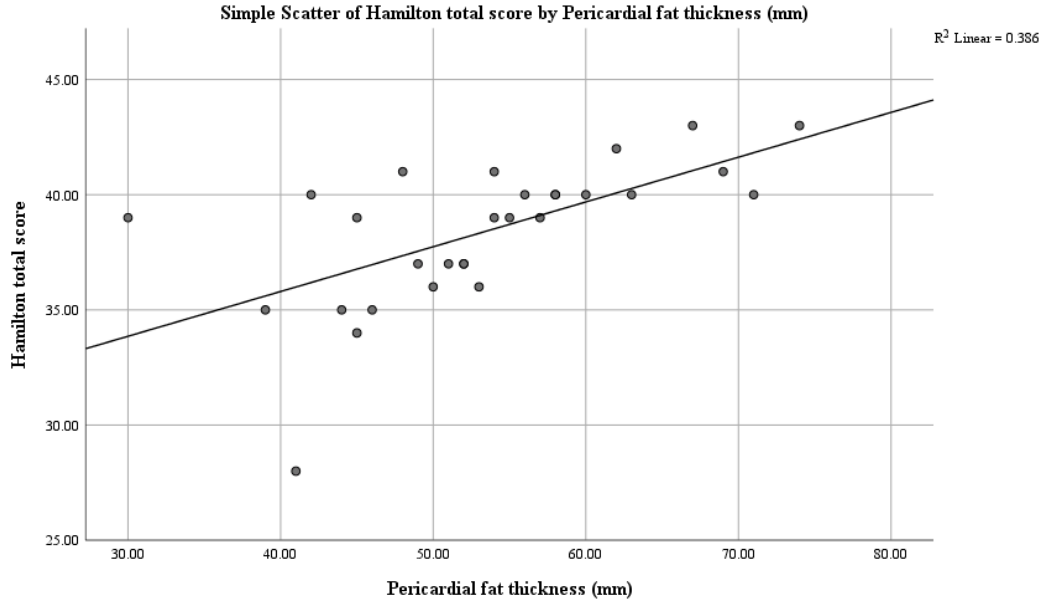

Figure 1. Scatterplot showing the association between pericardial fat thickness and Hamilton total score, with regression line

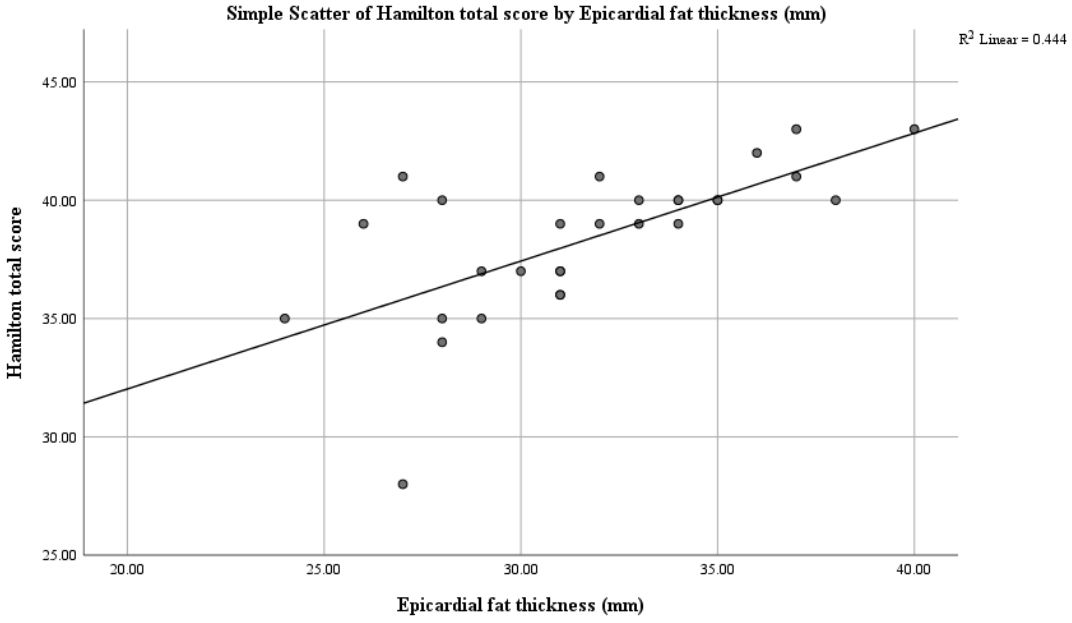

Figure 2. Scatterplot showing the association between epicardial fat thickness and Hamilton total score, with regression line

Regression analysis

A simple linear regression was used to examine whether pericardial fat thickness predicted the Hamilton total score.

The overall model was significant ($F(1, 27) = 16.98$, $p < 0.001$) and accounted for 38.6% of the variance ($R^2 = 0.386$, adjusted $R^2 = 0.363$).

Pericardial fat thickness was a significant positive predictor ($B = 0.194$, $SE = 0.047$, $\beta = 0.621$, $t = 4.12$, $p < 0.001$). The 95% confidence interval for the unstandardized coefficient ranged from 0.098 to 0.291, indicating a stable and meaningful effect (Figure 3).

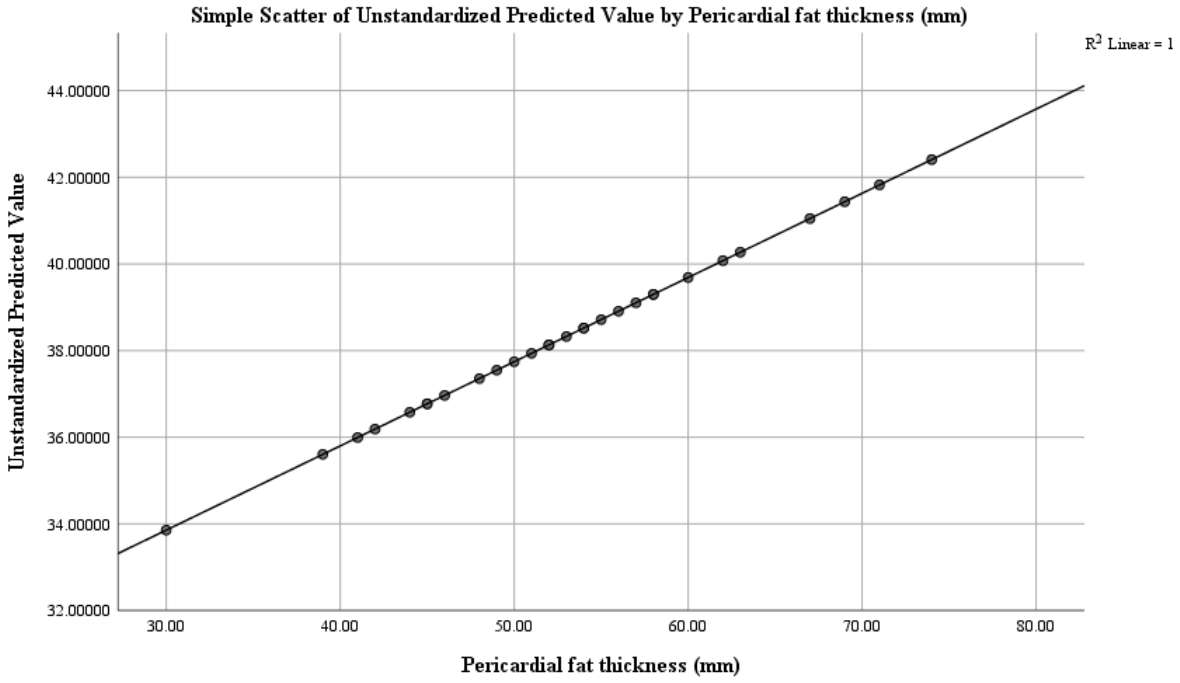

Figure 3. Hamilton total score predicted by the first regression model.

In addition, our second simple linear regression was conducted to determine whether epicardial fat thickness can predict the Hamilton total score measuring anxiety. The overall model was again significant ($F(1, 27) = 21.59$, $p < 0.001$) and accounted for 44.4% of the variance in Hamilton total score ($R^2 = 0.444$, adjusted $R^2 = 0.424$). Epicardial fat thickness emerged as a significant positive predictor ($B = 0.540$, $SE = 0.116$, $\beta = 0.667$, $t = 4.65$, $p < 0.001$). The robust effect was indicated by the fact that the 95% confidence interval for the unstandardized coefficient ranged from 0.302 to 0.779. Furthermore, no systematic bias in model predictions was demonstrated by the standard error of the estimate (2.39), and by the residuals, which ranged from –7.81 to 5.19, with a mean of 0.00 (Figure 4).

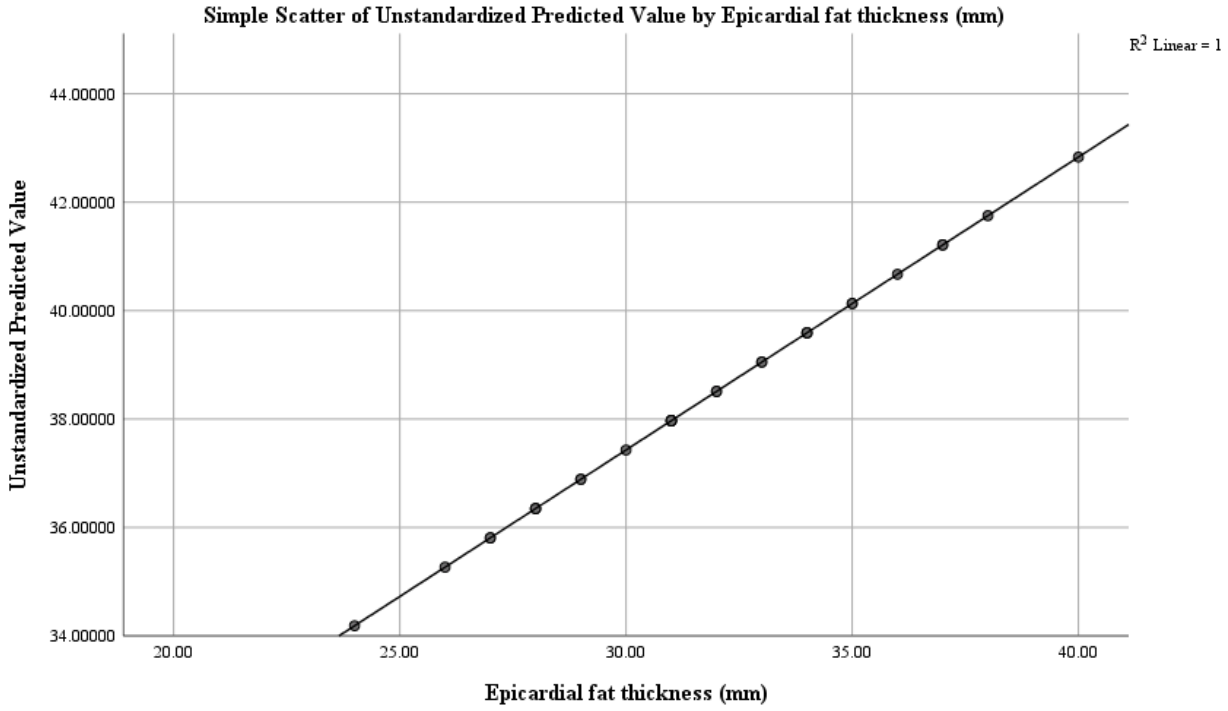

Figure 4. Hamilton total score predicted by the second regression model.

Group differences by obesity grade

A one-way analysis of variance (ANOVA) was conducted to compare cardiac adipose tissue thickness for the three BMI-based obesity categories. The obesity groups were as follows: Obesity Grade I (BMI 30.0–34.9; n = 6), Obesity Grade II (BMI 35.0–39.9; n = 14), and Obesity Grade III (BMI ≥ 40; n = 9). We had two distinct analyses, one for pericardial fat thickness and one for epicardial fat thickness.

The results of the ANOVA showed that pericardial fat thickness differed significantly across obesity grade groups. The mean values for each obesity group were: 45.83 mm (SD = 3.31) in Grade I, 50.36 mm (SD = 8.62) in Grade II, and 62.78 mm (SD = 8.26) in Grade III.

The ANOVA also indicated a significant effect of obesity grade, $F(2,26)=10.50$, $p < 0.001$. Post-hoc LSD comparisons showed that Grades I and II did not differ significantly (mean difference = –4.52 mm, $p = 0.243$), whereas Grade III had significantly higher pericardial fat thickness than both Grade I (mean difference = 16.94 mm, $p < 0.001$) and Grade II (mean difference = 12.42 mm, $p = 0.001$). Thus, the substantial increase in pericardial fat thickness occurred primarily in the transition to Grade III obesity (Figure 5).

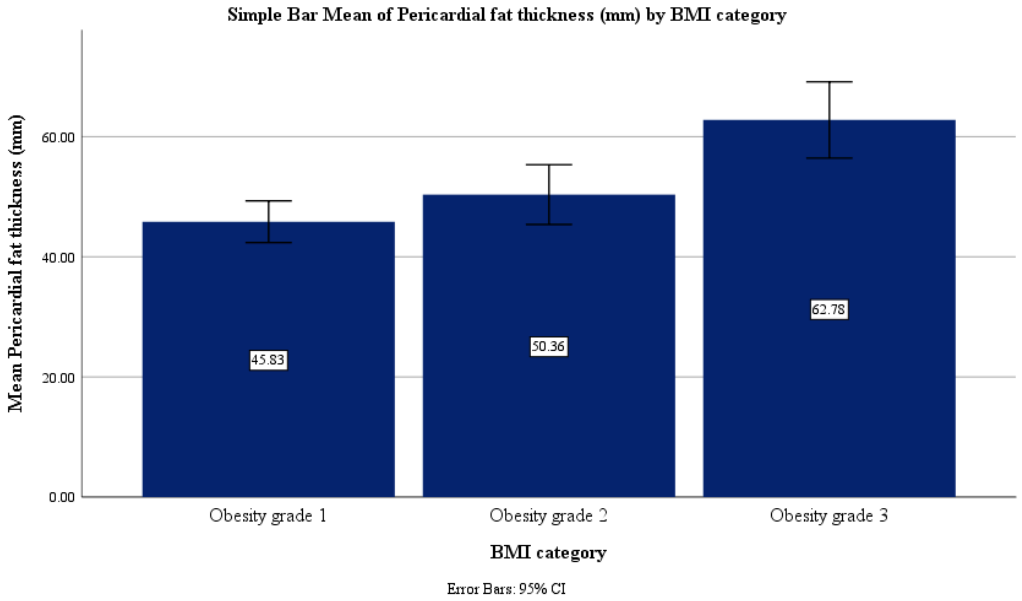

Figure 5. Mean pericardial fat thickness (mm) across the three BMI-based obesity categories. A one-way ANOVA showed a significant effect of obesity grade on pericardial fat thickness, $F(2,26)=10.50$, $p < 0.001$. Post-hoc LSD comparisons indicated that Obesity Grade III had significantly higher pericardial fat thickness than both Grade I (mean difference = 16.94 mm, $p < 0.001$) and Grade II (mean difference = 12.42 mm, $p = 0.001$), while no significant difference was observed between Grades I and II ($p = 0.243$).

The results of the ANOVA for epicardial fat thickness showed the same pattern. Mean values were 28.83 mm (SD = 1.47) in Grade I, 30.79 mm (SD = 3.12) in Grade II, and 35.22 mm (SD = 3.73) in Grade III. The ANOVA results again demonstrated a significant effect of obesity grade, $F(2,26)=9.02$, $p = 0.001$. Post-hoc LSD tests revealed no significant difference between Grades I and II (mean difference = –1.95 mm, $p = 0.207$), while Grade III exhibited significantly higher epicardial fat thickness than both Grade I (mean difference = 6.39 mm, $p = 0.001$) and Grade II (mean difference = 4.44 mm, $p = 0.002$). As with pericardial fat, epicardial fat thickness increased markedly only in the highest obesity category (Figure 6).

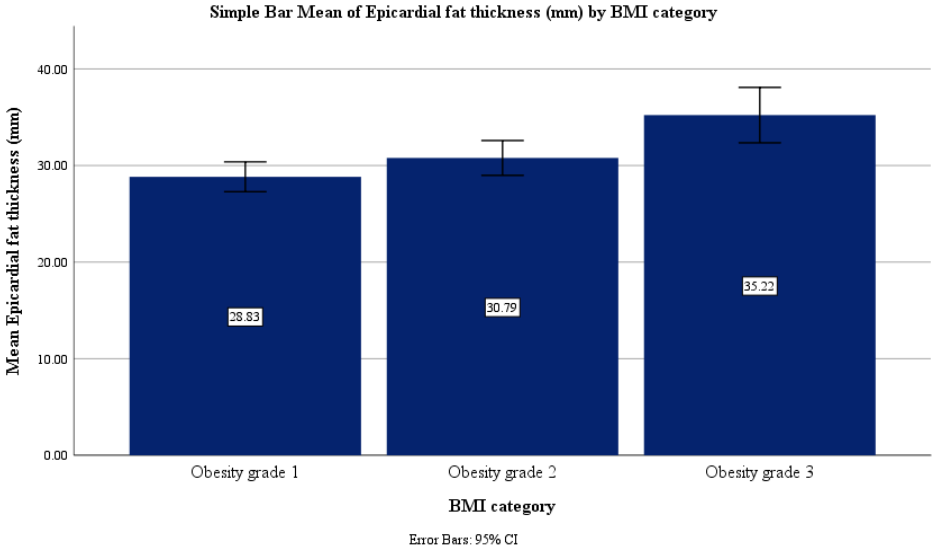

Figure 6. Mean epicardial fat thickness (mm) across the three obesity categories. The one-way ANOVA revealed a significant effect of obesity grade, $F(2,26)=9.02$, $p = 0.001$. Post-hoc LSD tests showed that Obesity Grade III had significantly higher epicardial fat thickness than both Grade I (mean difference = 6.39 mm, $p = 0.001$) and Grade II (mean difference = 4.44 mm, $p = 0.002$). Grades I and II did not differ significantly ($p = 0.207$).

4. Artificial Intelligence in the Assessment of Epicardial Adipose Tissue and Obesity: Methods, Architectures, and Performance

4.1. Recent Advances in Deep Learning–Based Segmentation and Quantification of Epicardial and Pericardial Adipose Tissue: A Systematic Review

Deep learning methods have seen a dramatic increase in popularity in recent years. These approaches have led to significant advances in cutting-edge performance in areas such as image analysis, speech recognition, and natural language processing.

ConvNets are a type of artificial neural network in which the hidden layers are made up of convolutional filters. These filters are designed to extract relevant features from the data. Depending on the size of the kernel, each neuron in a layer responds only to a certain portion of the previous layer, an area called the receptive field. The filters are applied to the entire input using the same weights, which allows the detection of the same feature regardless of its position in the input data and leads to the obtaining of a feature map.

Typically, convolutional layers are accompanied by activation functions, such as ReLU (Rectified Linear Unit), which introduce nonlinearity into the model, as well as pooling layers, which reduce the size of the data and help maintain translation invariance in the feature identification process.

The sample analysed in this study included 250 consecutive sets of non-contrast, ECG-synchronized CT images obtained for the standard assessment of coronary calcium (CAC) scoring. These data were randomly selected from the prospective EISNER study conducted at Cedars-Sinai Medical Center.

The patient group consisted of asymptomatic individuals with no known history of coronary artery disease but with cardiovascular risk factors. No studies were excluded from the analysis due to poor image quality or artifacts. On average, each examination included 55 transverse sections with a section thickness of 2.5 mm or 3 mm. Each axial section was 512×512 pixels, corresponding to a spatial resolution of 0.684 mm × 0.684 mm. In total, the study included 13,756 transverse images for analysis.

To evaluate the performance of the ConvNet procedure for quantifying epicardial adipose tissue (EAT), it was necessary to establish a reference standard. In this context, a cardiologist imaging physician, certified in cardiac CT and with more than 3 years of experience in interpreting CT examinations for coronary calcium score (CAC), manually drew closed contours on each axial section, in order to delimit the pericardium, including both the heart and the EAT.

Subsequently, a second closed contour was drawn, external to the first, to delimit the paracardial adipose tissue (PAT), located outside the pericardium. The segmentation process was performed using the semi-automated research software QFAT, developed at Cedars-Sinai Medical Center.

Based on these delimitations, corresponding binary masks were created for EAT and heart, for PAT, as well as a chest mask obtained by joining them. In accordance with the methodology described in the literature, a threshold was applied to eliminate pixels whose HU values did not fall within the fat attenuation range (−190 HU to −30 HU). Also, to reduce the impact of artifacts on the measurements, each section was processed by applying a median filter with a 3×3 kernel.

The adipose tissue segmentation process is performed on axial sections, which are introduced as input data into a first neural network, called Net1. This is based on a convolutional architecture, designed to extract and learn hierarchical features from the provided images.

As shown in Figure 7, first, fully connected (dense) layers are attached to the architecture, in order to establish whether the analysed section lies within the anatomical boundaries of the heart (Task 1). Second, at the level of the HCU unit within the convolutional architecture, an up-sampling procedure is applied to support two distinct segmentation processes: one aimed at identifying the reunion of intra- and extrapericardial structures (Task 2), by defining the thoracic mask, and another oriented towards their differentiation (Task 3), by delimiting the epicardial and paracardiac masks.

A novel element of the method is the integration of dense layers with up-sampling blocks, which allows the simultaneous optimisation of the same convolutional architecture for two types of tasks: section classification and segmentation itself.

The identification of the pericardium is then performed by a second neural network, called Net2. The epicardial mask obtained by the Net1 network is initially used to perform radial sampling and to convert the CT section from Cartesian coordinates to cylindrical coordinates. The thus transformed image is introduced into Net2, which generates a probability map corresponding to the pericardial sac. The maximum likelihood values are used to determine a contour, whose shape is adjusted and stabilized by a statistical shape model (SSM).

The statistical shape model was built by applying singular value decomposition (SVD) to contours manually drawn by specialists, in order to identify the main morphological variations. In the final stage, additional processing — including applying a HU threshold ([-190 HU, -30 HU]) to exclude pixels that do not correspond to adipose tissue, as well as median filtering — results in binary fat images, used for adipose tissue quantification.

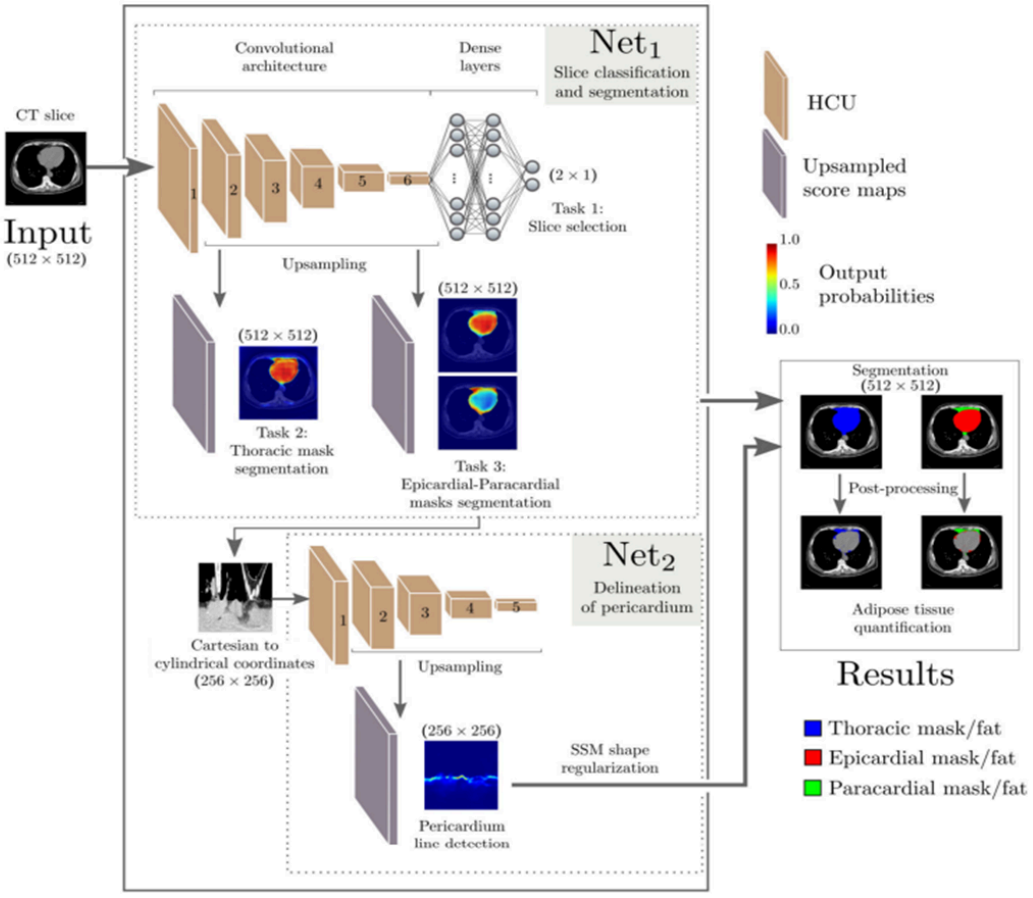

Figure 7. An axial slice is fed into the first network (Net1), which simultaneously performs three tasks: predicting whether the slice is within the heart boundaries, segmenting the thoracic mask, and segmenting the epicardial and paracardial masks. A second network (Net2) detects the pericardium line after transforming the input into cylindrical coordinates. Shape regularization (SSM) is then applied to obtain the final segmentation, followed by post-processing (Hounsfield unit thresholding and median filtering) to extract the adipose tissue. Adapted by Commandeur et al. (2018). Deep learning for quantification of epicardial and thoracic adipose tissue from non-contrast CT. IEEE Transactions on Medical Imaging, 37(8), 1835–1846. https://doi.org/10.1109/TMI.2018.2804799

The convolutional architecture implemented in Net1 consisted of six HCUs arranged in succession. Each unit included a convolution layer, followed by a ReLU activation function and a max-pooling layer.

The first HCU was responsible for extracting local texture information from the neighborhood of each pixel, using a 5×5 filter. A stride of 2 was used for both the convolution and max-pooling operations, reducing the input image resolution from 512×512 to 128×128. The other five HCUs had the same structure: they used a 3×3 convolutional kernel, with stride 1 for convolution and stride 2 for max-pooling. As one advances towards the deeper layers of the network, the size of the feature maps progressively decreases.

The upper layers integrated the global information from the previous maps, capturing anatomical organization and providing localization details. This information was then used in the slice selection process. To perform the section selection step (Task 1), fully connected (dense) layers were added to the convolutional architecture. The first two of these were connected to HCU 6 and each had 1024 neurons. Their role was to integrate and synthesize the information previously extracted by the convolutional network, generating two output values corresponding to the two possible classes: acceptance or rejection of the analyzed section.

Subsequently, a SoftMax layer was applied in order to transform the two raw scores into normalized probabilities. These indicate the chance that the evaluated axial section is inside or outside the anatomical limits of the heart. The final section selection decision was made by comparing the probability associated with falling within the limits of the heart with a predefined threshold. Once the input section was chosen, the results obtained from the binary mask-based segmentations (Tasks 2 and 3) were integrated into the analysis. The convolutional network architecture was extended by adding two upsampling modules. The first of these was responsible for segmenting the thoracic mask.

At the level of each unit, from HCU 2 to HCU 6, the feature maps were initially combined to produce a score map. More precisely, each pixel in this map was assigned the value resulting from a weighted sum of the corresponding pixels in all available feature maps. This weighted aggregation was implemented using a convolutional layer with a kernel of size F×1×1, where F indicates the total number of feature maps. In the next step, five successive upsampling layers were applied to return the score maps to the original resolution of the input data.

The performance of the model used for the classification of sections (Net1), in terms of determining their belonging to the anatomical boundaries of the heart, was analysed by means of ROC (Receiver Operating Characteristic) curves, built based on the test set for each of the 10 subsets (folds) of the cross-validation.

The results indicated an excellent capacity of the model in the selection process of the relevant sections, the average value of the area under the curve (AUC) being 0.992±0.002. The highest classification accuracy, of 0.953±0.005, was obtained at a decision threshold equal to 0.531±0.051. The model demonstrated accurate identification of cardiac boundaries, with average reported section positioning errors per examination of 0.22±0.287 for the lower boundary and 0.132±0.316 for the upper boundary, expressed in section units.

No misclassifications were observed in the mid-heart area or in regions located at considerable distance from its boundaries. There was also a slight superiority in performance in detecting the upper boundary compared to the lower boundary, reflected by a lower average error. The proposed method could represent a time-efficient tool for the fully automated determination of EAT and TAT in routine clinical practice. Integrated with calcium score assessment obtained from non-contrast CT scans, it could contribute to more accurate cardiovascular risk stratification, without additional radiation exposure for the patient or additional effort on the physician's part.

The time required for segmentation and quantification of volumetric adipose tissue is less than 26 seconds for a full 3D scan performed on a standard computer. In comparison, manual EAT and TAT assessment by a specialist takes approximately 10–11 minutes. This significant time difference may facilitate the integration of TAT and EAT volume quantification into routine clinical workflow, thus supporting a more efficient and accurate assessment of cardiovascular risk (Commandeur et al., 2018).

4.2. Dual U-Net–Based Automatic Segmentation and Quantification of Epicardial Adipose Tissue from CT Images with Integrated Morphological Processing

To achieve the most accurate segmentation and quantitative evaluation of epicardial fat, an innovative approach based on the U-Net architecture was proposed, which uses two consecutive U-Net networks, complemented by a morphological processing layer, applied to cardiac CT images. U-Net is one of the most widely used architectures in deep learning models for image segmentation, demonstrating remarkable performance, especially in the field of medical imaging. The general scheme of the proposed method is illustrated in Figure 8.

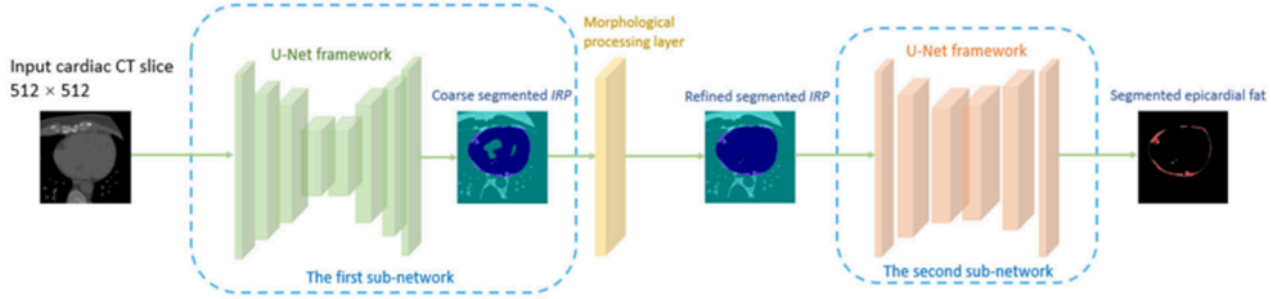

Figure 8. The complete pipeline of the proposed method consists of two sub-networks incorporating a morphological layer for the segmentation and quantification of epicardial fat
Adapted by Zhang et al. (2020). Automatic epicardial fat segmentation and quantification of CT scans using dual U-Nets with a morphological processing layer. IEEE Access, 8, 128032–128041. https://doi.org/10.1109/access.2020.3008190

The first sub-network, built based on the U-Net architecture, is responsable for identifying the pericardium before performing the segmentation of the inside region of the pericardium (IRP). However, the initial segmentation of the internal area may contain imperfections, such as gaps, irregular edges or small, noisy artifacts on the outside. To address these shortcomings, an additional morphological processing layer is added at the end of the first sub-network to refine the result and obtain an optimal internal delineation of the pericardium. The second sub-network takes the previously segmented IRP region and analyses it in order to identify and quantify epicardial fat.

The first sub-network configuration is based on the U-Net architecture, considered a widely used reference model for semantic segmentation tasks of medical images. This architecture is distinguished by two defining elements: its characteristic “U” shape and skip connections, illustrated in Figure 9.

The U-shaped design allows the extraction and integration of relevant semantic information about the segmented object at the level of the entire image, while highlighting its relationship to the context in which it is located. Therefore, this structure significantly contributes to the accurate identification and localization of the targeted objects.

At the same time, the skip link allows the transmission of high-resolution information from the encoder to the decoder corresponding to the same level. Through this mechanism, the fine details necessary for a more precise segmentation are preserved and exploited.

Therefore, the use of the U-Net architecture in medical image segmentation brings three essential benefits. First, the model proves to be stable and reliable even when trained on small datasets. Second, it is a high-performance, efficient solution for medical image segmentation, being able to achieve very good results. Third, its architecture is simple and well-structured, facilitating subsequent adaptation and optimization.

In Figure 9, the initial cardiac CT image used as input has a resolution of 512 × 512 pixels, and the result obtained is a binary mask of the same size, intended to delineate the inner pericardium area (represented by blue pixels). The outer area of the IRP (marked in green) is

assigned the value zero to simplify the subsequent processing steps through morphological operations.

The green lines illustrated in Figure 9 connect the encoder and decoder at the same level, facilitating the combination of features extracted from superficial layers with those from deep layers. To obtain the most accurate delimitation of the inner pericardium region, a morphological processing layer is applied to the approximate IRP generated by the first subnet.

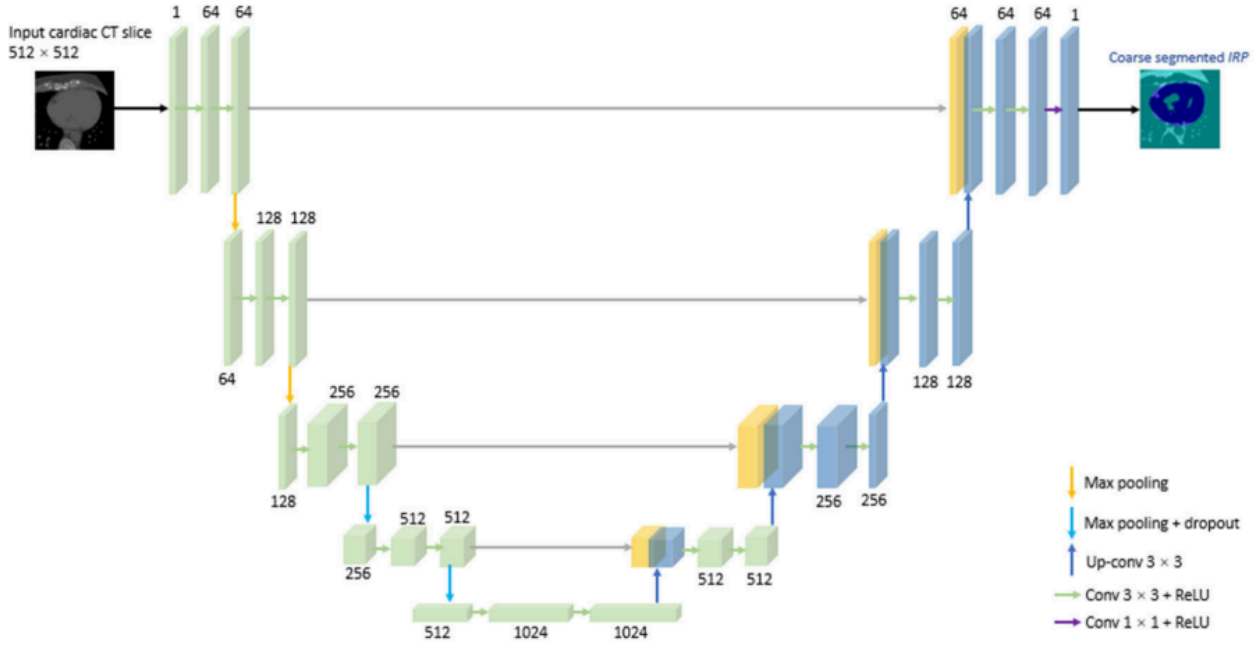

Figure 9. The architecture of the first sub-network. The yellow boxes indicate the feature maps used to combine with the corresponding feature maps (green boxes) after up-sampling. Adapted by Zhang et al. (2020). Automatic epicardial fat segmentation and quantification of CT scans using dual U-Nets with a morphological processing layer. IEEE Access, 8, 128032–128041. https://doi.org/10.1109/access.2020.3008190

For a more detailed examination and quantitative assessment of the epicardial fat identified in the segmented IRP at the morphological layer level of the first subnet, a second subnet was developed in this study. This network also uses a U-Net architecture. The input data consists of a segmented IRP with a size of 512 × 512 pixels, obtained by applying an optimised binary mask over the corresponding CT image. It is important to emphasize that the image introduced into the network is not a binary one, but represents the IRP region already segmented from the associated CT image, which is to be processed by the second subnet. The output generated by this second subnet consists of a segmentation of the epicardial fat, having the same dimensions as the input image.

The results demonstrate that the proposed method offers high performance in identifying IRPs, reaching values of 95.05% for the average Dice score and 91.14% for the average IOU. In the same comparative analysis, established segmentation methods such as FCN, U-Net and Seg-Net were also included. The proposed approach records the best results in segmenting and measuring epicardial fat, achieving 84.25% for the average IOU, 91.19% for the average Dice score and 0.9304 for the Pearson correlation coefficient.

This study demonstrated an innovative technique for identifying and measuring epicardial fat in cardiac CT images. The proposed method allows for delineation of the inner pericardial region, optimization of the mask of interest, and automated segmentation of epicardial fat. The

results demonstrate strong agreement with manual markings by specialists and significantly outperform other existing modern methods.

In conclusion, the presented solution can serve as an effective tool for reducing the time required for processing and segmenting epicardial fat, with promising prospects for integration into clinical practice (Zhang et al., 2020).

4.3. An Enhanced Deep Learning Method for the Quantification of Epicardial Adipose Tissue

The following study included 108 patients aged 48 to 70 years (mean ± standard deviation: 60.1 ± 6.0 years), of whom 62 (57.4%) were male. Participants underwent routine coronary computed tomography angiography (CCTA) examinations at the Second Xiangya Hospital of Central South University between April and September 2022. Subsequently, CCTA images were evaluated to determine epicardial adipose tissue (EAT) volume.

To develop and validate the deep learning algorithm, EAT identified on CCTA images was manually segmented in a group of 108 patients. The segmentations were performed by two radiologists with 3 and 5 years of experience. Subsequently, the results were independently reviewed by a specialist with 20 years of experience in cardiac surgery and a radiologist with 21 years of practice, until a final consensus was reached.

In the first step, two distinct labels were defined: one to delineate the pericardium together with its internal space and the other to identify EAT deposits. The pericardial contour, visible on the CCTA images, was manually traced, section by section, in the axial plane, and then the automatic filling of the delimited region was applied.

Epicardial adipose tissue was defined as tissue with fat characteristics located between the myocardium and the visceral pericardium, being identified based on attenuation values within the range [-190 HU, -30 HU].

In a first phase, a deep convolutional neural network (CNN), denoted Pθ, is designed and trained to automatically identify the pericardium in each contrast-enhanced CT image for the addressed segmentation task. The symbol θ denotes all the internal parameters of the model, adjusted during the training process. The fundamental role of the Pθ network is to perform image segmentation, separating the pericardial region from the image background.

To define the architecture, the Pθ model is implemented using the U-Net structure, known for its symmetrical “U”-shaped configuration. The original U-Net architecture was introduced by Ronneberger and his collaborators in the field of biomedical image segmentation.

The Pθ network is organized into two major components: the contracting path and the expansive path.

Both components of the network include a sequence of convolutional layers that apply zero-padding (3×3) dimensional filters, as well as unit-step (1×1) convolutions. After each convolutional step, Batch Normalization (BN) and the Rectified Linear Unit (ReLU) activation function are applied. To reduce spatial dimensions, the contracting path uses max-pooling (2×2) layers, thereby performing down-sampling. In addition, the expansive path uses transposed convolutions (2×2) to perform up-sampling and restore the original image resolution.

In the training phase, only CT sections in which the pericardium is present are used to allow the model to learn the specific characteristics of this anatomical structure. In contrast, in the testing phase, a complete series of CT images from real patients is analysed, which includes both sections containing the pericardium and sections in which it is not visible.

The training process of the Pθ network is carried out over 200 epochs, and the parameters are optimized by minimizing the L2 loss function.

To highlight the performance of the proposed algorithm for quantifying EAT, a series of numerical experiments was performed. The training stage was carried out in the COLAB environment, using a Tesla P100 GPU on a Linux operating system, with the implementation made

in PyTorch. In parallel, the proposed MIDL method was developed in Python 3.7 and run on a desktop computer equipped with an Intel Core i7-10700 processor.

For the 108 patients included in the study, the complete data set was built by correlating the contrast-enhanced CT matrices in their original form with the pericardial matrices manually labeled by specialists. The data were then divided into three distinct subsets: a training set of 60 cases (2205 contrast-enhanced CT sections), a validation set of 8 cases (361 contrast-enhanced CT sections), and a test set of 40 cases (1862 contrast-enhanced CT sections).

The training subset was used to train a modified version of the U-Net architecture. During the training process, we used the Adam optimizer in combination with the Xavier initialization method, working with a batch size of 5 and a learning rate set to 0.001. To maximize the use of available information and improve the generalization ability of the model, we applied data augmentation techniques to the initial CCTA images, including randomly generated rotations, flips, and translations.

The automated method showed a high level of agreement with the manual assessment performed by specialists, recording a median Dice coefficient (DSC) of 0.916 (interquartile range – IQR: 0.846–0.948) at the level of two-dimensional sections. Regarding the three-dimensional reconstructions, the median DSC value was 0.896 (IQR: 0.874–0.908), indicating a very good overlap between the two methods, supported by an excellent correlation of 0.980 ($p<0.001$) for EAT volumes.

Also, the Bland–Altman analysis applied to the model showed a low systematic deviation, with a bias of -2.39 cm^3. The integration of pericardial anatomical landmarks within the deep learning algorithms contributes significantly to the optimization of the automatic quantification of EAT. The obtained performances underline the potential of the method for use in clinical practice (Tang et al., 2024).

4.4. Deep Learning (DL) and Support Vector Machines (SVMs) in Obesity Prediction

Dugan et al. applied machine learning methods to predict the onset of obesity in early childhood. The research used both supervised and unsupervised learning techniques, such as K-means, DT, and SVM, to develop a model based on computational intelligence. To compare the performance of the methods, several evaluation metrics were considered, including precision, recall, true positive class rate, false positive rate, and area under the ROC curve. After the data preprocessing stage, which included identifying missing values, detecting outliers, and analyzing correlations — the model training and classification processes were performed. The results show that the DT method, together with the Simple K-means algorithm, achieved superior performance in terms of precision (98.5%), recall (98.5%), true positive rate (98.5%), false positive rate (0.2%), and ROC area (99.5%), thus surpassing previous studies, which reported accuracy levels between 75% and 85%.

Shcherbatyi's study is a relevant new example of the effective use of predictive models in a therapeutic context. The authors aimed to estimate the success of a six-month weight loss intervention, analyzing a group of 20 Swiss children, aged 11 to 16, who were overweight or obese. Among the variables used for prediction were body weight, age, body mass index (BMI), height, resting heart rate values, as well as several heart rate measurements recorded both during a running test and during the recovery phase after exercise. Several machine learning algorithms were experimented with for modeling, including KNN, Gradient Boosting (GB), decision trees (DT), and support vector machines (SVM). Given the small number of participants, the researchers applied nested cross-validation to ensure rigorous internal evaluation and adequate training of the models. The best-performing model, based on a linear SVM, achieved an accuracy rate of 85%. Permutation test analyses indicated that heart rate-related variables made the largest contribution to the model's predictive ability. In addition, the performance of the machine learning models exceeded the estimates made by two experts in the field.

Montañez and his team identified genetic variants in the participants' profiles using data science methods, and these variants were subsequently classified as risk variants in the National Human Genome Research Institute's Catalog. Many machine learning methods for predicting obesity use indexed genetic variants or single-nucleotide polymorphisms (SNPs) as input variables. A conducted study analyzed the use of machine learning techniques in estimating obesity risk based on available genetic profiles. To assess susceptibility to chronic hepatitis based on SNP data, the SVM, decision tree, decision rule, and KNN algorithms were implemented. Among all the methods tested, SVM demonstrated the best predictive model performance. Simulation results indicated that SVM achieved the highest area under the curve (AUC) value, reaching 90.5%.

Three of the most widely used AI methods for estimating obesity risk are neural networks, decision trees, and logistic regression. Decision trees can capture nonlinear relationships between variables and provide easy-to-follow classification rules. In contrast, logistic regression generates clear, interpretable results, highlighting relevant risk factors. All of these approaches are valuable in AI-assisted obesity studies because neural networks are particularly effective at detecting subtle patterns in complex data sets and often provide superior predictive performance (Shabani Jafarabadi & Busetto, 2025).

5. Discussion

This study examined how different measures of body fat relate to anxiety symptoms in adults with obesity. The results of the statistical analysis showed a clear and consistent pattern. Participants with higher levels of adiposity tended to report higher anxiety scores. This was true for general measures such as BMI and waist circumference, and it was also true for more specific measures such as abdominal wall thickness. The strongest associations appeared for cardiac adipose tissue thickness. Both pericardial and epicardial adipose tissue thickness showed strong positive correlations with the Hamilton Anxiety Rating Scale total score. These findings suggest that individuals with greater fat accumulation, especially around the heart, tend to experience higher levels of anxiety.

The regression analyses supported this interpretation. Pericardial and epicardial adipose tissue thickness each predicted Hamilton total score on their own. Both models explained a meaningful amount of the variance in anxiety symptoms. The regression coefficients were stable and precise, and the residuals showed no systematic pattern. This means that the models performed well and that the relationship between cardiac fat and anxiety was not due to random variation. The predicted-value plots also showed a clear linear trend, with higher cardiac adipose tissue thickness corresponding to higher predicted anxiety scores.

Furthermore, the group comparisons by obesity grade added another important observation. Pericardial and epicardial adipose tissue thickness increased steadily from Grade I to Grade III obesity. However, the largest increase occurred in Grade III. Participants in this group had much thicker cardiac adipose tissue layers than those in the other two groups. Grades I and II did not significantly differ from each other. This pattern suggests that the most severe level of obesity is associated with a sharper rise in cardiac fat accumulation. Because cardiac fat thickness was also linked to anxiety, this may help explain why individuals with more severe obesity tend to show higher anxiety scores.

Overall, the findings of this study indicate that anxiety symptoms are closely related to several markers of adiposity. The strongest relationships were observed for cardiac adipose tissue thickness. Although the study cannot determine whether adiposity causes anxiety, the consistent associations across all analyses suggest that these factors are meaningfully connected. The results highlight the importance of considering both psychological and physiological aspects when evaluating individuals with obesity.

The pattern observed in this study aligns with previous work showing that obesity is closely linked to higher levels of anxiety. Large epidemiological studies have reported that individuals with obesity have a greater likelihood of experiencing anxiety symptoms than those with a normal

weight (Hamilton, 1959). Several authors have suggested that this relationship may be driven by both biological and psychological factors, including inflammation, autonomic imbalance, and the emotional burden associated with chronic illness (Milaneschi et al., 2019). The positive correlations we found between BMI, waist circumference, abdominal wall thickness, and Hamilton total score are consistent with these earlier findings (Hamilton, 1959; Milaneschi et al., 2019).

Research on cardiac fat has traditionally focused on physical health outcomes. Many studies have shown that epicardial and pericardial adipose tissue are associated with cardiometabolic risk, coronary artery disease, and systemic inflammation (Iacobellis, Corradi, & Sharma, 2005). These adipose tissue depots are metabolically active and release inflammatory mediators that can influence cardiovascular function. Although most research on obesity has focused on its physical complications, some studies suggest that inflammation and autonomic nervous system dysfunction may also contribute to anxiety symptoms (Vogelzangs et al., 2013). The strong associations we observed between cardiac adipose tissue thickness and the Hamilton total score support this idea. These findings also indicate that cardiac adipose tissue may be relevant for psychological outcomes as well.

The regression results in this study are consistent with findings reported in earlier studies. Previous research has shown that epicardial adipose tissue is a strong predictor of metabolic and cardiovascular complications, even after adjusting for BMI (Mahabadi et al., 2009). Our results show a similar pattern, but with anxiety as the outcome. Both pericardial and epicardial adipose tissue thickness predicted Hamilton total score, and each model explained a meaningful proportion of the variance. This suggests that cardiac adipose tissue may have effects that go beyond traditional cardiometabolic pathways and may also relate to emotional or stress-related processes.

The increase in cardiac adipose tissue observed across obesity grades follows the same trajectory noted in prior investigations. Other studies have demonstrated that the transition from moderate to severe obesity is associated with a sharp increase in metabolic and cardiovascular risk (Flegal et al., 2013). In our sample, pericardial and epicardial adipose tissue thickness increased across obesity grades, with the largest differences observed in Grade III. This mirrors the pattern described in the literature, where the highest obesity class often shows the steepest rise in various health risks. In addition, because cardiac adipose tissue thickness was also linked to anxiety, this may help explain why individuals with severe obesity often report higher psychological distress.

Finally, very few studies have examined the relationship between cardiac adipose tissue and anxiety directly. Most research on anxiety in obesity has focused on general adiposity, body image, or metabolic markers (Scott et al., 2008). By including detailed imaging measures of pericardial and epicardial adipose tissue, this study adds new important information to this line of research. It suggests that cardiac adipose tissue may be an important biological factor to consider when studying anxiety in people with obesity. This finding opens the door for future work that examines whether reducing visceral or cardiac adipose tissue through weight loss or lifestyle interventions may also influence anxiety symptoms.

These findings are also important when viewed from a bariatric perspective. Individuals who seek bariatric surgery often present with high levels of both physical and psychological burden. Many studies have shown that anxiety symptoms are common in bariatric candidates and that emotional distress can influence eating behavior, treatment adherence, and postoperative outcomes (Malik et al., 2014). The strong associations we observed between anxiety and several adiposity measures fit well with this clinical picture. They suggest that the psychological difficulties seen in bariatric patients may be linked not only to social or behavioral factors, but also to underlying biological changes related to fat accumulation.

Cardiac adipose tissue thickness is rarely discussed in routine bariatric evaluations, yet our results indicate that it may be relevant. Bariatric patients often have advanced forms of obesity, and many of them fall into the highest obesity grade. In our sample, participants in Grade III had the thickest pericardial and epicardial fat layers. This is consistent with previous research showing that severe obesity is associated with rapid increases in visceral and cardiac fat (Garg et al., 2023).

Because these adipose tissue depots were also linked to anxiety, it is possible that the biological stress associated with severe obesity contributes to the emotional difficulties commonly reported by bariatric patients.

The bariatric literature also shows that weight loss after surgery leads to reductions in visceral fat, improvements in inflammation, and better cardiovascular function (Kubik et al., 2013). Some studies have reported improvements in anxiety and depression after bariatric surgery as well. The present findings offer a possible explanation for this pattern. If cardiac adipose tissue thickness is related to anxiety, then reductions in cardiac fat after surgery may contribute to psychological improvement. This idea has not been tested directly, but it provides a useful direction for future research.

Another point to consider is that bariatric patients often experience long-standing obesity, repeated weight loss attempts, and chronic stress. These factors may amplify the relationship between adiposity and anxiety. The strong correlations observed in this study may therefore reflect the combined effects of biological vulnerability and psychological stress. This interpretation is consistent with previous work showing that bariatric candidates often have higher levels of emotional distress than individuals with obesity in the general population (de Zwaan et al., 2011).

Overall, the findings of this study fit well within the bariatric literature. They show that anxiety in bariatric patients is closely associated with several markers of adiposity, especially cardiac adipose tissue thickness. Our results also suggest that psychological assessment in bariatric care should consider not only behavioral and emotional factors, but also the biological characteristics of severe obesity. Future studies could examine whether reductions in cardiac adipose tissue after surgery are accompanied by reductions in anxiety, which would help clarify the exact direction of this association.

6. Conclusion

This study shows that the level of anxiety in bariatric patients is closely linked to several markers of adiposity, especially the thickness of epicardial and pericardial fat. Higher cardiac fat levels were strongly associated with higher Hamilton Anxiety scores, and these adipose tissue layers also increased sharply in the most severe obesity grade. These results suggest that both psychological and biological factors contribute to the emotional burden experienced by bariatric candidates. Understanding this connection may help improve preoperative assessment and guide more integrated care for patients with severe obesity.

References

Commandeur, F., Goeller, M., Betancur, J., Cadet, S., Doris, M., Chen, X., Berman, D. S., Slomka, P. J., Tamarappoo, B. K., & Dey, D. (2018). *Deep learning for quantification of epicardial and thoracic adipose tissue from non-contrast CT*. IEEE Transactions on Medical Imaging, 37(8), 1835–1846. https://doi.org/10.1109/TMI.2018.2804799

Flegal, K. M., Kit, B. K., Orpana, H., & Graubard, B. I. (2013). Association of all-cause mortality with overweight and obesity using standard body mass index categories: a systematic review and meta-analysis. *JAMA*, *309*(1), 71–82. https://doi.org/10.1001/jama.2012.113905

Garg, U. K., Mathur, N., Sahlot, R., Tiwari, P., Sharma, B., Saxena, A., Jainaw, R. K., Agarwal, L., Gupta, S., & Mathur, S. K. (2023). *Abdominal fat depots and their association with insulin resistance in patients with type 2 diabetes*. PLOS ONE, 18(12), e0295492. https://doi.org/10.1371/journal.pone.0295492

Gariepy, G., Nitka, D., & Schmitz, N. (2010). *The association between obesity and anxiety disorders in the population: A systematic review and meta-analysis*. International Journal of Obesity, 34(3), 407–419. https://doi.org/10.1038/ijo.2009.252

Guh, D. P., Zhang, W., Bansback, N., Amarsi, Z., Birmingham, C. L., & Anis, A. H. (2009). *The incidence of co-morbidities related to obesity and overweight: A systematic review and meta-analysis*. BMC Public Health, 9, 88. https://doi.org/10.1186/1471-2458-9-88

Hamilton, M. (1959). *The assessment of anxiety states by rating*. British Journal of Medical Psychology, 32(1), 50–55. https://doi.org/10.1111/j.2044-8341.1959.tb00467.x

Hruby, A., & Hu, F. B. (2015). *The epidemiology of obesity: A big picture*. Pharmacoeconomics, 33, 673–689. https://doi.org/10.1007/s40273-014-0243-x

Iacobellis, G. (2015). *Local and systemic effects of the multifaceted epicardial adipose tissue depot*. Nature Reviews Endocrinology, 11(6), 363–371. https://doi.org/10.1038/nrendo.2015.58

Iacobellis, G., Corradi, D., & Sharma, A. M. (2005). Epicardial adipose tissue: anatomic, biomolecular and clinical relationships with the heart. *Nature clinical practice. Cardiovascular medicine*, *2*(10), 536–543. https://doi.org/10.1038/ncpcardio0319

Kubik, J. F., Gill, R. S., Laffin, M., & Karmali, S. (2013). The impact of bariatric surgery on psychological health. *Journal of obesity*, *2013*, 837989. https://doi.org/10.1155/2013/837989

Lavie, C. J., Milani, R. V., & Ventura, H. O. (2009). *Obesity and cardiovascular disease: Risk factor, paradox, and impact of weight loss*. Journal of the American College of Cardiology, 53(21), 1925–1932. https://doi.org/10.1016/j.jacc.2008.12.068

Luppino, F. S., de Wit, L. M., Bouvy, P. F., Stijnen, T., Cuijpers, P., Penninx, B. W., & Zitman, F. G. (2010). Overweight, obesity, and depression: a systematic review and meta-analysis of longitudinal studies. *Archives of general psychiatry*, *67*(3), 220–229. https://doi.org/10.1001/archgenpsychiatry.2010.2

Mahabadi, A. A., Massaro, J. M., Rosito, G. A., Levy, D., Murabito, J. M., Wolf, P. A., O'Donnell, C. J., Fox, C. S., & Hoffmann, U. (2009). *Association of pericardial fat, intrathoracic fat, and visceral abdominal fat with cardiovascular disease burden: The Framingham Heart Study*. European Heart Journal, 30(7), 850–856. https://doi.org/10.1093/eurheartj/ehn573

Malik, S., Mitchell, J. E., Engel, S., Crosby, R., & Wonderlich, S. (2014). Psychopathology in bariatric surgery candidates: a review of studies using structured diagnostic interviews. *Comprehensive psychiatry*, *55*(2), 248–259. https://doi.org/10.1016/j.comppsych.2013.08.021

Milaneschi, Y., Simmons, W. K., van Rossum, E. F. C., & Penninx, B. W. (2019). Depression and obesity: evidence of shared biological mechanisms. *Molecular psychiatry*, *24*(1), 18–33. https://doi.org/10.1038/s41380-018-0017-5

Ng, M., Fleming, T., Robinson, M., Thomson, B., Graetz, N., Margono, C., Mullany, E. C., Biryukov, S., Abbafati, C., Abera, S. F., Abraham, J. P., Abu-Rmeileh, N. M. E., Achoki, T., AlBuhairan, F. S., Alemu, Z. A., Alfonso, R., Ali, M. K., Ali, R., Alvis Guzman, N., … Gakidou, E. (2014). *Global, regional, and national prevalence of overweight and obesity in children and adults during 1980–2013: A systematic analysis for the Global Burden of Disease Study 2013*. The Lancet, 384(9945), 766–781. https://doi.org/10.1016/S0140-6736(14)60460-8

Powell-Wiley, T. M., Poirier, P., Burke, L. E., Després, J. P., Gordon-Larsen, P., Lavie, C. J., Lear, S. A., Ndumele, C. E., Neeland, I. J., Sanders, P., St-Onge, M. P., & American Heart Association Council on Lifestyle and Cardiometabolic Health. (2021). *Obesity and cardiovascular disease: A scientific statement from the American Heart Association*. Circulation, 143(21), e984–e1010. https://doi.org/10.1161/CIR.0000000000000973

Rosito, G. A., Massaro, J. M., Hoffmann, U., Ruberg, F. L., Mahabadi, A. A., Vasan, R. S., O'Donnell, C. J., & Fox, C. S. (2008). Pericardial fat, visceral abdominal fat, cardiovascular disease risk factors, and vascular calcification in a community-based sample: the Framingham Heart Study. *Circulation*, *117*(5), 605–613. https://doi.org/10.1161/CIRCULATIONAHA.107.743062

Scott, K. M., McGee, M. A., Wells, J. E., & Oakley Browne, M. A. (2008). Obesity and mental disorders in the adult general population. *Journal of psychosomatic research*, *64*(1), 97–105. https://doi.org/10.1016/j.jpsychores.2007.09.006

Shabani Jafarabadi, G., & Busetto, L. (2025). *Artificial intelligence in obesity prevention*. Healthcare, 13, 3262. https://doi.org/10.3390/healthcare13243262

Tang, K.-X., Liao, X.-B., Yuan, L.-Q., He, S.-Q., Wang, M., Mei, X.-L., Zhou, Z.-A., Fu, Q., Lin, X., & Liu, J. (2024). *An enhanced deep learning method for the quantification of epicardial adipose tissue*. Scientific Reports, 14, 24947. https://doi.org/10.1038/s41598-024-75659-9

Toader, M., Gheorghe, L., Chirica, C., Ghicu, I.-A., Chirica, S.-I., Mazga, A. I., Haba, D., Maxim, M., Miler, A. A., Crișu, D., Haba, M. Ș. C., & Timofte, D. V. (2025). *Cardiovascular profile and cardiovascular imaging after bariatric surgery: A narrative review*. Medicina, 61(1), 73. https://doi.org/10.3390/medicina61010073

Vogelzangs, N., Beekman, A. T., de Jonge, P., & Penninx, B. W. (2013). Anxiety disorders and inflammation in a large adult cohort. *Translational psychiatry*, *3*(4), e249. https://doi.org/10.1038/tp.2013.27

World Health Organization. (2021). *Obesity and overweight*. https://www.who.int/news-room/fact-sheets/detail/obesity-and-overweight

Zhang, Q., Zhou, J., Zhang, B., Jia, W., & Wu, E. (2020). *Automatic epicardial fat segmentation and quantification of CT scans using dual U-Nets with a morphological processing layer*. IEEE Access, 8, 128032–128041. https://doi.org/10.1109/access.2020.3008190

de Zwaan, M., Enderle, J., Wagner, S., Mühlhans, B., Ditzen, B., Gefeller, O., Mitchell, J. E., & Müller, A. (2011). Anxiety and depression in bariatric surgery patients: a prospective, follow-up study using structured clinical interviews. *Journal of affective disorders*, *133*(1-2), 61–68. https://doi.org/10.1016/j.jad.2011.03.025